



Electrochemical stability of gold complex based on mercaptotriazole at optimal condition

Stevan P. Dimitrijević¹ · Silvana B. Dimitrijević² · Aleksandra Ivanović² · Nikola Vuković³ · Nikhil Dhawan⁴

Received: 30 April 2022 / Accepted: 24 August 2022
© Institute of Chemistry, Slovak Academy of Sciences 2022

Abstract

This study investigates the electrochemical stability of the gold complex based on mercaptotriazole at an optimum pH of nine in the electrolyte with a gold concentration of 2.5 g dm^{-3} . The stability of the complex was studied by visual monitoring and electrochemical characterization of electrolytes over a period of 1 year. Electrochemical characterization of the mercaptotriazole gold complex was performed using open circuit potential measurement, cyclic voltammetry, recording the polarization curves, pH, and conductivity of the electrolyte. Electrochemical characteristics and visual appearance of the mercaptotriazole gold complex at a pH ~ 9 were not significantly changed for one year, with no changes in its visual appearance. The results of this study are important for industrial applications in order to replace cyanide electrolytes with a stable organic complex.

Keywords Gold organic complex · Mercaptotriazole · Electrochemical stability · Electroplating · Coatings

Introduction

Gold coatings are mentioned as the first galvanic coatings from 1800 with first patent on the gold deposition in 1840. The patent describes the application layer of gold on silver from a solution of alkaline cyano-aurates by electric current and is designated as the beginning of galvanic gilding (Đorđević 1990). Gold coatings (hard and soft) are used in the electronics (Đorđević 1990; Đorđević et al. 1998; Okinaka and Hoshino 1998) and jewelry industry due to their excellent electrical conductivity and high corrosion resistance (Hemsley and Green 1991; Roy 2009; Hosseini and Ebrhimi 2010).

Cyanide electrolytes, mainly used for the deposition of gold coatings, are extremely stable (stability constant 10^{38}), but they are highly toxic, poor compatibility with positive

photoresist effects, and high wastewater treatment costs (Okinaka and Hoshino 1998; Rapson and Groenewald 1978; Traut et al. 1990; Honma and Hagiwara 1995). Due to this reason, and especially in modern times, there is a trend of using electrolytes based on some organic compounds without cyanides content. However, their usage has not satisfied industry use due to the low stability constant, demonstrated by the complex destruction and gold precipitation from electrolytes (Dimitrijević et al. 2013; Xingkai et al. 2020).

This is the main reason for the interest in developing non-toxic gold electrolytes (Liew et al. 2003; Green and Roy 2006). Non-cyanide baths are reported in the literature such as sulfite and amino-sulfite baths (Okinaka and Hoshino 1998; Rapson and Groenewald 1978; Honma and Hagiwara 1995; Dauksher et al. 1994), Au(I) thiosulfate baths (Okinaka and Hoshino 1998; Kato and Okinaka 2004; Sullivan and Kohl 1997), thiosulfate-sulfite baths (Roy 2009; Kato and Okinaka 2004; Kato et al. 2002; Krulik and Mandrich 1993), baths based on thiourea (Kato and Okinaka 2004; Krulik and Mandrich 1993), baths with ascorbic acid (Inoue et al. 1999; Sato et al. 2002), bath without reducing agent (Sato et al. 2002; Luo et al. 2018), Au(III) halide baths (Luo et al. 2018; Dimitrijević et al. 2015), Au(I) thiomalate baths (Kato and Okinaka 2004; Sullivan and Kohl 1997), other baths and research about organic gold complex based on mercaptotriazole (Dimitrijević et al. 2013, 2014, 2015, 2016, 2019, 2021).

✉ Silvana B. Dimitrijević
silvana.dimitrijevic@irmbor.co.rs

¹ Innovation Center of Faculty of Technology and Metallurgy, University of Belgrade, Belgrade, Serbia

² Mining and Metallurgy Institute Bor, Zelene bulevar 35, Bor 19210, Serbia

³ Institute for Technology of Nuclear and Other Mineral Raw Materials, Belgrade, Serbia

⁴ Indian Institute of Technology, Roorkee, India

A significant problem in non-cyanide electrolytes for gilding is their low stability manifested by the disintegration of the complex and the deposition of elemental gold. Cyanide baths are very stable, while non-cyanide electrolytes show varying degrees of instability that make their use limited. The instability of non-cyanide baths is usually manifested by the formation of colloidal gold, which is usually attributed to the reaction of disproportionation of Au (I) ions in solution (Honma and Hagiwara 1995; Sullivan and Kohl 1997):

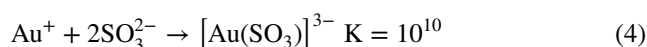
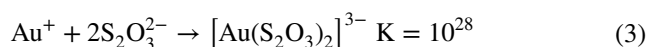
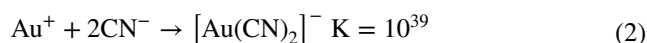


The formation of colloidal gold is an undesirable phenomenon in the gilding process because of their increased surface roughness leading to the formation of nodules and other defects (Baumgärtner et al. 1997). The surface of gold particles can cause additional autocatalytic gold deposition, which accelerates the decomposition of the baths (Roy 2009). In extreme cases, gold deposition was also observed on the surfaces of the galvanizing cell due to their instability.

Oxidation of ligands (e.g., sulfites to sulfates) tends to increase the concentrations of other less stable Au(I) complexes and reduce the overall stability of the bath. Similarly, hydrolysis, ligand exchange, and protonation reactions can lead to the formation of unstable forms of gold, which can negatively affect the stability of the bath (Green 2007).

Theoretical

The standard potentials versus the normal hydrogen electrode (NHE) for a variety of Au(I) and Au(III) complexes are given in Table 1 (Osaka et al. 2006; Qu et al. 2014; Richter et al. 1989; Garcia and Burleigh 2013). The most important ion for electrodeposition is $[\text{Au}(\text{CN})_2]^-$. The stability of the Au(I) cyanide complex is reflected in the shift of the reduction potential for Au(I) from 1.71 (aquo complex) to -0.611 V (cyanide complex). The stability constants for three gold complexes of interest for electrodeposition are given below (Inoue et al. 1999; Dimitrijević et al. 2013).



The potentials for the reduction of Au(III) to Au and Au(III) to Au(I), as shown in Table 1, are important

Table 1 Standard reduction potentials for gold ions (V vs. NHE) (Okinaka and Hoshino 1998)

Half reactions	Potential, V
Au(I) \rightarrow Au	
$\text{Au}^+ + e^- \rightarrow \text{Au}$	1.71–1.85
$[\text{AuCl}_2]^- + e^- \rightarrow \text{Au} + 2\text{Cl}^-$	1.15
$[\text{AuBr}_2]^- + e^- \rightarrow \text{Au} + 2\text{Br}^-$	0.96
$[\text{AuI}_2]^- + e^- \rightarrow \text{Au} + 2\text{I}^-$	0.58
$[\text{Au}(\text{SCN})_2]^- + e^- \rightarrow \text{Au} + 2\text{SCN}^-$	0.66
$[\text{Au}(\text{S}_2\text{O}_3)_2]^{3-} + e^- \rightarrow \text{Au} + 2\text{S}_2\text{O}_3^{2-}$	0.15
$[\text{Au}(\text{CN})_2]^- + e^- \rightarrow \text{Au} + 2\text{CN}^-$	–0.61
Au(III) \rightarrow Au	
$\text{Au}^{3+} + 3e^- \rightarrow \text{Au}$	1.71–1.85
$[\text{AuCl}_4]^- + 3e^- \rightarrow \text{Au} + 4\text{Cl}^-$	1.00
$[\text{AuBr}_4]^- + 3e^- \rightarrow \text{Au} + 4\text{Br}^-$	0.85
$[\text{AuI}_4]^- + 3e^- \rightarrow \text{Au} + 4\text{I}^-$	0.56
$[\text{Au}(\text{SCN})_4]^- + 3e^- \rightarrow \text{Au} + 4\text{SCN}^-$	0.64
Au(III) \rightarrow Au(I)	
$\text{Au}^{3+} + 2e^- \rightarrow \text{Au}^+$	1.40
$[\text{AuCl}_4]^- + 2e^- \rightarrow [\text{AuCl}_2]^- + 2\text{Cl}^-$	0.92
$[\text{AuBr}_4]^- + 2e^- \rightarrow [\text{AuBr}_2]^- + 2\text{Br}^-$	0.80
$[\text{AuI}_4]^- + 2e^- \rightarrow [\text{AuI}_2]^- + 2\text{I}^-$	0.55
$[\text{Au}(\text{SCN})_4]^- + 2e^- \rightarrow [\text{Au}(\text{SCN})_2]^- + 2\text{SCN}^-$	0.62

Table 2 Bath composition and operating conditions of Au-MT electrolyte (Dimitrijević et al. 2014, 2016)

Bath constituent	Au-mercaptotriazole
Gold concentration/(g dm ⁻³)	2.5
pH	9
Temperature/°C	22
Time/s	105
Cathode current density/(A dm ⁻²)	1
Current intensity/A	0.12
Voltage/V	3.5

because Au(III) can also be used as the source of gold in baths in place of Au(I) and Au(III) can be formed at the anode during plating through the oxidation of Au(I).

Electrolyte stability was examined over 12 months by visual monitoring of changes and determination of electrochemical characteristics in the observed period. The smallest changes were observed in electrolytes with pH = 9 (Dimitrijević et al. 2018).

The gold complex based on mercaptotriazole was investigated in this work (Table 2), with electrochemical stability as the main subject.

Electrochemical characterization of gold complexes with mercaptotriazole was performed for the solution with $\text{pH}=9$ in the following time intervals: 1 h, 4 h, 24 h, 48 h, 7 days, 1 month, 3 months, 6 months, 9 months, and a year (1 month in the study was defined as a period of 30 days). The pH value and conductivity of the gold-mercaptotriazole (Au-MT) electrolyte were also monitored during this period. Additionally, turbidity measurements were performed over the 2 months.

Experimental

Chemicals

For the synthesis of the gold complex with mercaptotriazole, the following chemicals were used: gold powder (99.99%, Mining and Metallurgy Institute Bor); hydrochloric acid p.a. (Zorka, Šabac); nitric acid p.a. (Zorka, Šabac); glycine (min. 99%, Alkaloid, Skopje); potassium hydroxide (Merck, Germany); double distilled water (conductivity $\sim 1 \mu\text{S}/\text{cm}$), and mercaptotriazole. Mercaptotriazole was synthesized in our laboratory. Thiosemicarbazide, $\text{CH}_5\text{N}_3\text{S}$ (min 98%, Merck, Germany) and formamide p.a. (Alkaloid, Skopje) were used in this synthesis. Synthesis was performed as per reported procedure (Dimitrijević et al. 2013). A large quantity of Au-MT electrolyte was synthesized and divided into 100 mL portions using volumetric flasks for further electrochemical experiments.

Out of 10 isomers of mercaptotriazole (Fig. S1), only three forms can be synthesized by this procedure (Fig. S2). All three are tautomeric, having an SH-substituted 1,2,4-triazole structure (Holm and Straub 2011), and they can readily interconvert. At pH of 9, glycine forms a zwitterion (Altinkaya et al. 2020) and typically forms an O,O-chelate complex with gold, in the same manner as with other transitional metal cations (e.g. Remko and Rode 2006; Das and Mandal 2015). In the reaction with chloroauric acid (Dimitrijević et al. 2013), mercaptotriazole and glycine thus form a complex with presumably square planar coordination of Au(III) (Fig. S3). Such molecular geometry allows a formation of hydrogen bonds between the acidic NH-protons of mercapto-1,2,4-triazoles (Ji Ram et al. 2019) and the oxygen atoms of zwitterionic glycine, which may additionally improve the stability of the Au-MT complex.

Electrochemical and physicochemical characterization

Electrochemical studies were performed in a custom-made system consisting of an electrochemical cell and hardware interface for computerized control and data acquisition and reported elsewhere (Dimitrijević et al. 2013, 2018).

In a standard thermostated three-electrode electrochemical cell, the working electrode was a gold-plated platinum electrode (surface area 4.5 mm^2), and its potential was controlled against the reference electrode (saturated calomel electrode (SCE)—Radiometer Analytical XR110 Reference Electrode). All electrochemical potentials are related to this reference electrode ($+241 \text{ mV}$ vs. SHE, standard hydrogen electrode; same for normal hydrogen electrode) and platinum foil (2.0 cm^2) served as a counter electrode.

The pH of the electrolyte was measured with the pH meter, model pH 3310 (WTW, Germany). A Hanna HI-991301 conductivity meter (Hanna Instruments, Portugal) was used to measure the conductivity of samples. Turbidity of the electrolyte was measured with WTW Lab Turbidity Meter Turb[®] 550 IR (WTW, Germany).

The temperature of $25 \pm 0.1 \text{ }^\circ\text{C}$ and 100 mL of the electrolyte was maintained in all the experiments. The pH and conductivity of the electrolytes were measured before and after each electrochemical measurement. Before the start of each experiment, the electrochemical cell was rinsed twice with distilled water followed by working solution. The open-circuit potential (OCP) was monitored for a period of 600 s, of which the first 300 s and beyond that OCP changes were insignificant.

Cyclic voltammograms were recorded with a scan rate of 100 mV s^{-1} , in the range of potential from 0.0 to -1.0 V , with control for 7 days old electrolyte, where the bottom limit was extended to -1.2 V to illustrate the start of the gaseous hydrogen evolution, which starts at about -1.15 V .

Polarization curves were recorded with a scan rate of 5 mV s^{-1} in the potential range from $+0.4$ to -1.3 V in the cathodic direction. The potential range was limited for the same reason as for cyclic voltammetry for the bottom of the range and the theoretical potential for the evolution of gaseous oxygen ($+0.454 \text{ V}$ as calculated value) for the upper limit. However, only a range from 0.0 to -1.3 V was presented since it was mostly the cathodic part for all polarization curves, which was of the main interest in this study.

Results and discussion

Visual monitoring of electrolyte

Freshly synthesized electrolyte with the gold concentration of 2.5 g dm^{-3} and $\text{pH}=9$ is pale yellow, almost colorless. Any visual changes were not observed by monitoring the electrolyte with $\text{pH} \approx 9$ for one year.

Figure 1 shows the insignificant change in the appearance of the electrolyte in the entire investigated period.

The electrolyte stability was additionally tested by a simple test with ether (Inoue et al. 1999). Adding the ether to the complex of gold based on mercaptotriazole

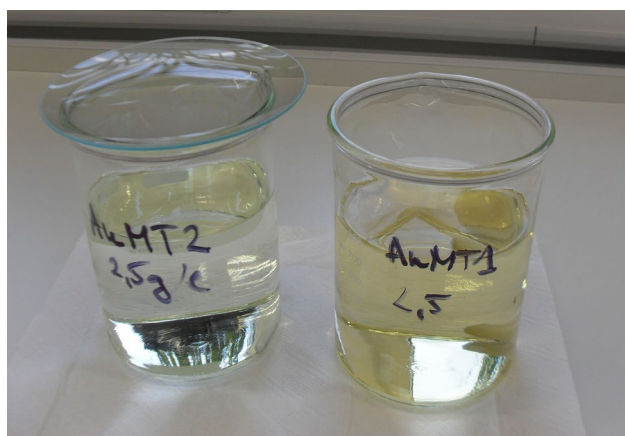


Fig. 1 The visual appearance of electrolyte: left: after one year, right: fresh electrolyte

Table 3 Turbidity of electrolyte in the period of two months

Time from the synthesis	Turbidity/NTU
1 h	0.14
4 h	0.20
24 h	0.24
48 h	0.26
7 days	0.29
1 month	0.31
2 months	0.36

brings the ether, as lighter, to the surface of the mixture. It remains colorless, which means that the gold was still in the complex based on mercaptotriazole as more stable than ether complex.

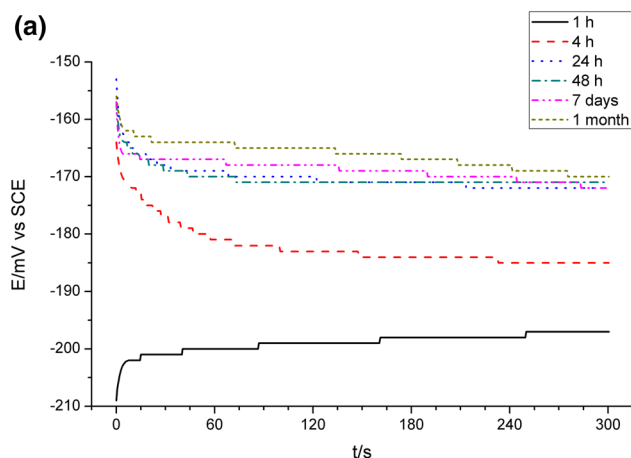


Fig. 2 Open circuit potential value measured for the gold complex based on mercaptotriazole at pH=9 and $C_{Au}=2.5 \text{ g/cm}^3$ for the different elapsed times after the electrolyte synthesis: **(a)** from 1 h to

The electrolyte stability was compared with the electrochemical stability of the gold cyanide complex $K_2[Au(CN)_2]$. It is known that the cyanide complex of gold decomposes in acids with the evolution of hydrogen cyanide gas. The gold complex's stability based on mercaptotriazole was examined by adding diluted hydrochloric, nitric, and sulfuric acids. However, no significant visual changes in the electrolyte (clarity, color, precipitate, etc.) or gas evolution were noted with the addition of these acids.

Additionally, the electrolyte's turbidity was measured over 2 months. Results are given in Table 3.

Changes in electrolyte turbidity during 2 months were insignificant. Turbidity was far lower than 1.00 in the whole period and thus invisible to the naked eye. Values in the table are corrected and given after subtraction of turbidity of the double distilled water.

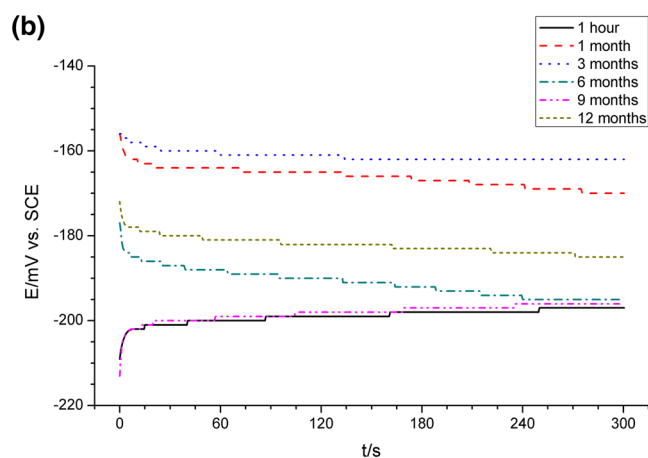
Open circuit potential

Figure 2 shows the curves of the open circuit potential of the electrolytes after:

- 1 h, 4 h, 24 h, 48 h, 7 days, and 1 month;
- 1 h, 1 month, 3 months, 6 months, 9 months, and 12 months.

Note: after the initial period, OCP values were rounded to a millivolt with the aim to accentuate the fast stabilization of the measured potential and to avoid small variations (tenths of mV or smaller).

The stable value of OCPs for all elapsed time after the electrolyte synthesis was established almost immediately



7 days and 1-month (as the control) **(b)** from 1 month to 12 months, and 1 h (as the control)

after the immersion of the electrode, as can be seen in Fig. 2. Also, it can be noted that the change of pH value over time was insignificant. In all measurements, the initial periods with a sharp change in OCP value were very short, 5–10 s, and from there, OCP was very stable. The period for full stabilization was 60–120 s, and such a short period is the feature of this electrolyte and was observed ever again from the first study of the complex (Dimitrijević et al. 2013).

Table 4 shows the measured values of open circuit potential (after 300 s), pH value, and conductivity of electrolyte before and after electrochemical measurements after 1 h, 4 h, 24 h, 48 h, 7 days, 1 month, and then every month from the time of synthesis up to a year.

Table 4 shows almost identical values for the OCP for the age of electrolyte from 48 h to 2 months and between 3 and 5 months. Very similar values are also after the age of 6 months with two levels of OCP (about -185 mV and -195 mV) in that period. This strongly suggests high electrochemical stability of the complex. The similarities in this parameter are even more pronounced in Fig. 2a, where the electrolyte age curves from 48 h to a week partially overlap. In practical terms, these curves are identical in this full period. For the age of a month, the difference is negligible. This indicates that the structure of the complex is stable after 48 h. This stability is evident in the first 2 months. After a slight deviation after 3 months, the complex behaves almost identical up to the 5 months and then again small variation between 5 and 6 months. In the period from 6 to 12 months, two intervals lasting 3 months (6–9 and 10–12) were almost

the same in the OCP value. Overall, this parameter could be considered nearly constant for the whole year.

Figure 2b shows a great similarity between the one-hour and nine-month-old electrolytes curves, as well as the endpoints for both, as well as the six-month-old electrolyte, which practically coincides.

Figure 2 and Table 4 show that the most negative value of open circuit potential (-0.197 V) was measured 1 h after the electrolyte synthesis. The most positive OCP of -0.161 V was obtained after 4 months. After 4 h from the synthesis, OCP gets the value of -0.185 V that has not been changed much in a prolonged period, and the measured values of the open circuit potential, after 4 h and after one year, are equal: -0.185 V. However, the positive shift of 13 mV in the period between 4 and 24 h was recorded, which can be related to the small changes in the complex structure in the first 24 h, similar to other characteristics of the electrolyte (Dimitrijević et al. 2015, 2018). The greater difference (-32 mV) was between values measured after 5 months and 6 months. In the absolute sense, it was a small change (for a month) and should not be connected with any instability issue. Since the electrolytes were tempered at 25 °C before measurements, the seasonal temperature variation in the laboratory could not be a direct cause. However, since the electrolyte was not tempered constantly, some minor variation in the complex structure may be temperature influenced, considering that the period was in the wintertime and that an hour of tempering is not enough to reverse them. Nevertheless, these changes could indicate significant

Table 4 Open circuit potential, pH value, and conductivity of electrolyte before and after electrochemical measurements for different standing time from the moment of synthesis

Time from the synthesis	OCP/V	pH (before)	pH (after)	Electrolyte conductivity/ $(\mu\text{S cm}^{-1})$ (before)	Electrolyte conductivity/ $(\mu\text{S cm}^{-1})$ (after)
1 h	-0.197	8.96	8.85	8045	8050
4 h	-0.185	8.80	8.70	8041	8048
24 h	-0.172	8.75	8.68	8040	8046
48 h	-0.171	8.72	8.65	8038	8045
7 days	-0.172	8.70	8.64	8035	8041
1 month	-0.170	8.75	8.68	8038	8044
2 months	-0.169	8.80	8.70	8040	8045
3 months	-0.162	8.87	8.79	8043	8049
4 months	-0.161	8.84	8.80	8039	8045
5 months	-0.163	8.83	8.80	8037	8044
6 months	-0.195	8.82	8.79	8036	8043
7 months	-0.197	8.81	8.77	8037	8043
8 months	-0.185	8.80	8.75	8037	8042
9 months	-0.196	8.78	8.74	8036	8042
10 months	-0.184	8.78	8.75	8036	8043
11 months	-0.189	8.77	8.74	8036	8044
12 months	-0.185	8.75	8.70	8035	8043

changes in the structure of the gold complex and should be probed further.

The pH value was very stable during the entire period of a year. After an initial drop (in the first 24 h) by 0.16, pH was constant at 8.80 with minimal variations, up to +0.07 and -0.10. Table 4 shows a decrease up to 1 month, then some increase till 3 months after synthesis, and finally slow decrease till the end of the measurement period (after a year). The differences in pH value before and after measurement of OCP were typically 0.05 and maximal of 0.11 for the freshly made complex. The electrolytes were hermetically sealed, but OCP experiments were performed in contact with air, so a slight decrease in pH could be due to the carbon dioxide solution in the electrolyte during the 10 min of OCP measurement and 5–10 min for manipulation with the aged electrolyte.

Finally, the conductivity of the electrolytes was almost constant, which strongly suggests the electrochemical stability of the electrolyte, especially when considering that no additives were used. Conductivity was about 8 mS cm^{-1} and had a regular but insignificant rise after the measurement of OCP value ($5\text{--}10 \text{ }\mu\text{S cm}^{-1}$). Correlation between conductivity and pH was expected (rise in the first parameter with higher pH), although the change in conductivity was relatively smaller. Both of these parameters had no direct correlation with the OCP value.

Cyclic voltammetry

Figure 3 shows voltammograms for different age of the Au-MT electrolyte.

Figure 3a displays a high similarity of the curves for different ages of the electrolyte. This is especially pronounced for curves after 1 h, 24 h, and 48 h with almost identical

peak values at about -0.97 V , with a slight decrease in its value with time and insignificant (within a few mV) shift towards more positive potentials. In the cathode direction, the curves for 1 h and 24 h almost coincide in the larger part, while in the anodic direction, the curves for 24 h and 48 h overlap in one part. The curve of 7 days aged electrolyte differs somewhat, where the peak occurs at a slightly more positive potential (around -0.94 V). It should be emphasized here that this curve was performed to the lower limit of the cathode potential, -1.2 V , compared to -1.0 V for others. This was done to make the graph clearer and show that the peak below -1 V was the gold reduction peak (its deposition on the working electrode), while hydrogen evolution begins at slightly more negative potentials (approximately -1.15 V). Additionally, the appearance of inflection points can be observed on cyclic voltammograms (CV), which for a solution 1 h after synthesis appears at a potential of -0.8 V , shifts to a more negative value of potential in 24 h, and appears at -0.85 V and 48 h from the synthesis of the solution at a potential of -0.9 V .

A significantly different curve is obtained for the electrolyte 4 h old when there is no pronounced peak, but some irregular shoulder is visible on the curve between -0.8 V and -0.9 V . Tiny peak at -0.9 V could be observed, but it was barely noticeable. This could imply that minor changes in the structure of the complex occur after a few hours of synthesis. After 24 h, a steady state is reached, which is probably identical to that of the freshly made complex; this is in line with the behavior of OCP values, as well as with the previously mentioned research of this complex.

Figure 3b reveals a high similarity of cyclic voltammograms for electrolyte age from 1 month to a full year. Although these curves are somewhat different from the line for an hour-old complex, they were still analogous. The

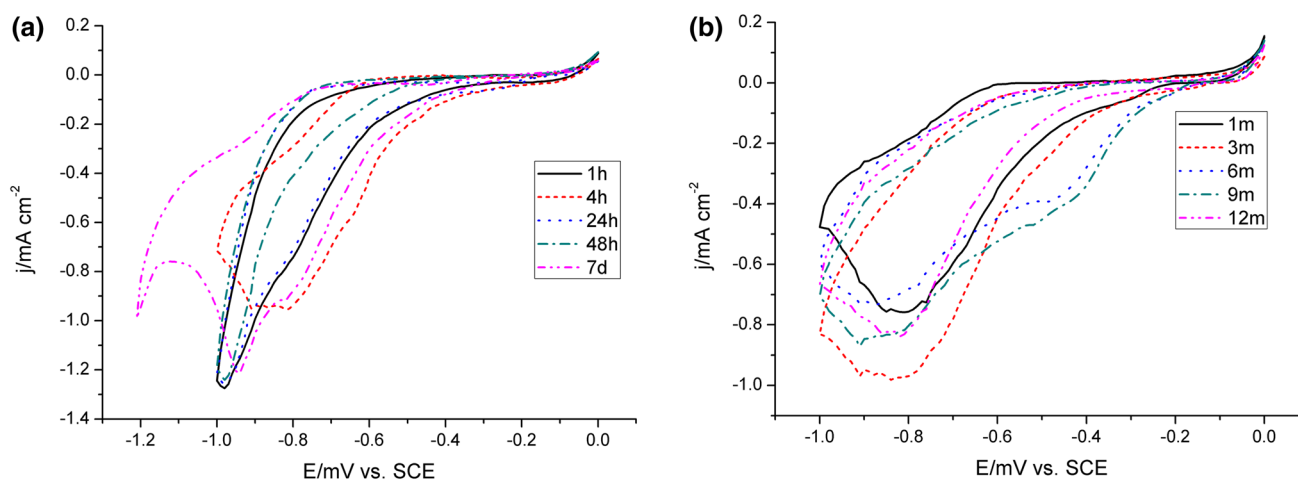


Fig. 3 Cyclic voltammograms for electrolyte concentration of 2.5 g/dm^3 at $\text{pH}=9$, as a function of time: (a) 1 h; 4 h; 24 h; 48 h and 7 days (168 h), and (b) 1 month; 3 months; 6 months, 9 months, and 12 months

main difference is that CVs for the older complexes had no prominent peaks. However, they share this property with the complex solution that was one week old, which strongly indicates a new form of the gold complex from a week after synthesis and onward. Maximum current densities in these longer periods were lower than for the age shorter than a week, but without significant differences. All the voltammograms had very pronounced shoulders at the potentials between -0.8 V and -0.9 V. A small and barely visible peak appeared in the diagram, at about -0.91 V, on the curves of the electrolytes 3–9 months old. These peaks were at the same potential and somewhat more positive than on the curves for the first 2 days after synthesis. Peaks and shoulders were consistent with the potential and correlated with the reduction potential of the complex (reduction of gold at the working electrode).

Polarization measurements

Figure 4 shows the polarization curves for an electrolyte with a concentration of 2.5 g dm^{-3} and $\text{pH}=9$ as a function of time.

Polarization curves in Fig. 4 show the excellent electrochemical stability of the tested electrolyte. The diagram shows three significant features: a two broad plateaus on the curves and peak appearance. These features can be interpreted as follows:

- the first plateau on the curves in Fig. 4 should represent adsorption of the gold complex, e.g., according to the deprotonation of the triazole rings ($\text{Au-MT} - 2\text{H}^+ \rightarrow \text{Au-MT}_{(\text{ads.})}$), which is a proven way of AMT (3-amino-5-mercapto-1,2,4-triazole) adsorption on the gold surface (cathode in this work) when applying an

appropriate electrode potential (Wrzosek and Bukowska 2007).

- the second plateau and the following peak indicate that the reduction of Au^{3+} complex ion could be a two-step process; the first step (the second plateau at more negative potentials) probably corresponds to the electrode reaction $\text{Au}^{3+}_{(\text{ads.})} \rightarrow \text{Au}^+$ and the second step (only peak on all curves) to the reaction $\text{Au}^+ \rightarrow \text{Au}_{(\text{s})}$, similar to the reduction of other Au(III) complex ions, like $\text{H}[\text{AuCl}_4]$ or THP-Au(III), (De Sá et al. 2011 and Jin et al. 2019, respectively).

In Fig. 4a, the clear peak can be observed at the potential of -0.93 or -0.94 V for all curves for electrolyte age from 24 h onwards. The curve for 1 h also had the peak at -0.95 V, but it was lower in intensity and had less width compared to the previous ones. The four hours aged electrolyte was similar to the previous, but the peak was further less pronounced. A decrease in the current density intensity at the same potentials is the next characteristic for the aging of the electrolyte in the first few hours. It was complementary to the findings of previous methods and strongly indicated some change in the gold complex structure. The appearance of the plateau on all curves in the diagram is their main property.

The wide plateaus (between -0.5 and -0.65 V) correspond to the limiting current densities (diffusion-controlled deposition of Au) explained in the previous study (Dimitrijević et al. 2013). The only significant deviation is observed with electrolytes after 24 h of synthesis, where this limiting current was the highest. However, it is not of great importance since the part of this curve overlaps some of the other, especially the one that corresponds age of electrolyte by 1 month. Additionally, 48 h of the synthesis had

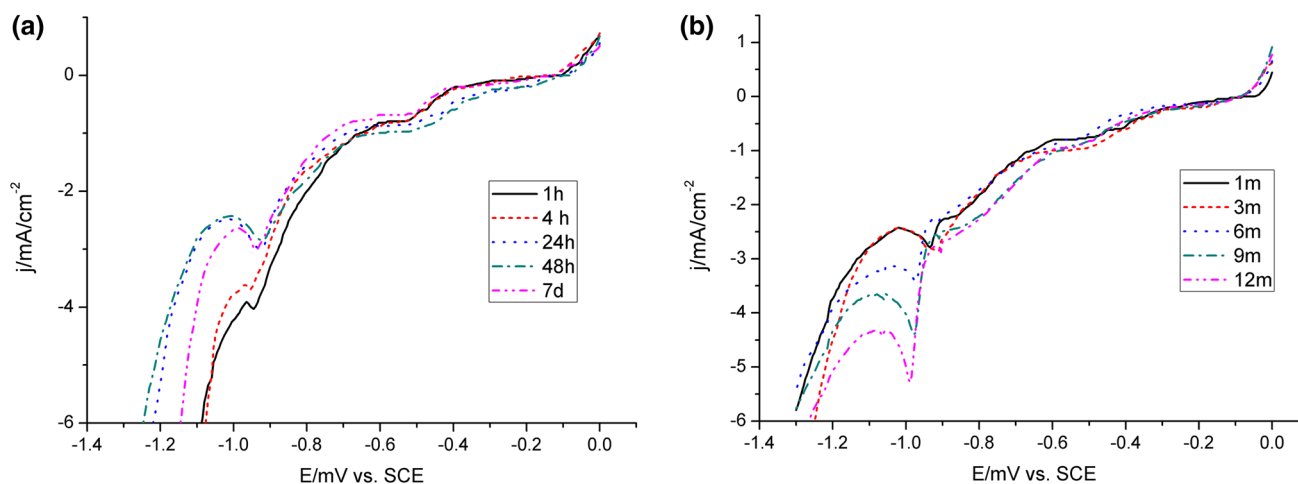


Fig. 4 Polarization curves for electrolyte concentration 2.5 g/dm^3 and $\text{pH}=9$, for the scan rate of 5 mV/s as a function of time, (a) for a period from 1 h to 7 days, (b) from for a period from 1 to 12 months

an almost identical polarization curve even with the limiting current closer to the electrolytes after one and 4 h from synthesis.

Figure 4a shows further similarity for electrolyte age of 1 month and more. Compared to Fig. 4b, the main differences are the more prominent peaks at the polarization curves for 6 months and afterward and lower limiting current densities. Nevertheless, the values of limiting current densities were similar, and the area for the limiting currents was nearly the same (from -0.5 to -0.65 V). In this interval, curves for 3, 9, and 12 months are similar, while one-month and 6 months curves are almost identical. However, at more negative potentials, similarity from 1 to 6 months is obvious, and between 9 and 12 months, it was continued down to the area of the pronounced peaks. Here, one-month and three-month-old electrolytes have given nearly the same response in the current.

In contrast, electrolytes 6, 9, and 12 months after the synthesis have behaved differently, giving clear peaks in the diagram. While peaks for the 1 month and 3 months are at the potential of -0.93 V, shifting to more negative potentials with the time from synthesis was regularity. Similar, the consistency in the peak intensity was the same (increase with the duration after synthesis). An interesting feature of these curves (6–12 months) was the appearance of the low-intensity pre-peaks and post-peaks. Nevertheless, it was beyond the topic of this paper and would be studied in detail in some future research.

Generally, whole Fig. 4 shows adequate similarity in polarization curves at different stages of electrolyte aging to strongly indicate the electrochemical stability of the gold complex during a year time.

Finally, the voltage of the electrolytic cell (gold plating of plates 40×25 mm from nickel-plated brass, distance between anode and cathode of 50 mm) measured for fresh electrolyte and 12 months old are compared and shown in Fig. 5.

Very similar electrolytic cell voltages are obtained for the time distance of the entire year. Shapes of the curves were nearly the same, and the maximal difference during 300 s of electroplating was 0.10 V and 0.13 V for the fresh and the old electrolyte, respectively.

In both cases, very solid voltage stability is obtained. The duration of the electroplating was calculated to obtain a $1.0 \mu\text{m}$ thick coating with assumed 95% current efficiency. Electric current efficiencies during electroplating were 96.84% for the newly synthesized electrolyte and 94.65% for 12 months aged one.

Although the electrochemical stability of the electrolyte cannot be proven with these limited sets of measurements under galvanostatic conditions, they indicate such a conclusion. A detailed galvanostatic decomposition study is certainly required for more detailed determination of the

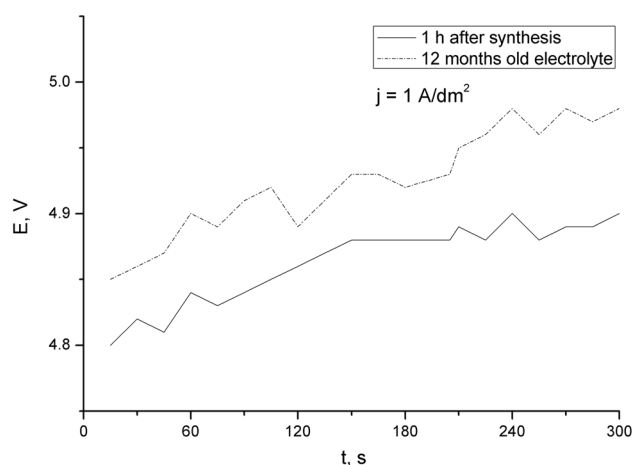


Fig. 5 Comparison of the electrolytic cell voltages between the fresh and 12-month-old electrolytes

electrochemical stability of the complex in galvanostatic conditions.

Conclusions

The Au-MT electrolyte at technically optimal pH value of nine was tested with different methods for one year to compare some of its significant characteristic change during that period. The study has shown:

1. no significant changes in any of the investigated parameters between the fresh electrolyte and after one year
2. minor differences between one and 4 h after synthesis of the gold complex and further to the 24 h, which implicate some minor changes in its structure;
3. almost identical behavior for 24 h and 48 h aged electrolyte and similar when compared 1 month and 3 months after synthesis;
4. the high similarity for the electrolyte age of 6, 9, and 12 months;
5. an indication of almost perfect electrochemical stability in the first 3 months after synthesis and good electrochemical stability up to 1 year.

This paper provides a solid basis for future studies of electrochemical stability with the use of additives and electrochemical characterization of the electrolyte in anodic area, which would eventually enable the industrial use of the tested gold complex. A comprehensive and rigorous galvanostatic decomposition study is necessary to prove the full stability of the gold complex under the conditions of industrial application. That will be the subject of further research.

Supplementary Information The online version contains supplementary material available at <https://doi.org/10.1007/s11696-022-02447-y>.

Acknowledgements Ministry of Education, Science and Technological Development of the Republic of Serbia, contract numbers: 451-03-68/2022-14/200052; 451-03-68/2022-14/200135; 451-03-68/2022-14/200023; COST Action CA20130; India-Serbia Bilateral Scientific and Technological Cooperation: Recycling of valuable metals from discarded printed circuit boards.

References

- Altinkaya P, Wang Z, Korolev I, Hamuyuni J, Haapalainen M, Kolehmainen E, Yliniemi K, Lundström M (2020) Leaching and recovery of gold from ore in cyanide-free glycine media. *Miner Eng* 158:106610. <https://doi.org/10.1016/j.mineng.2020.106610>
- Baumgärtner ME, Raub ChJ, Gabe DR (1997) Assessment of surface cleanliness for metal surfaces using an electrochemical technique. *Trans Inst Met Finish* 75:101–107. <https://doi.org/10.1080/00202967.1997.11871152>
- Das G, Mandal S (2015) Zwitterionic structures of selenocysteine-containing dipeptides and their interactions with Cu(II) ions. *Chem Pap* 69:616–626. <https://doi.org/10.1515/chempap-2015-0064>
- Dauksher WJ, Resnick DJ, Johnson WA, Yanof AW (1994) A new operating regime for electroplating the gold absorber on x-ray masks. *Microelectron Eng* 23:235–238
- De Sá AI, Eugénio S, Quaresma S, Rangel CM, Vilar R (2011) Electrodeposition of gold thin films from 1-butyl-1-methylpyrrolidinium dicyanamide Au³⁺ solutions. *Thin Solid Films* 519:6278–6283. <https://doi.org/10.1016/j.tsf.2011.03.135>
- Dimitrijević S, Rajčić-Vujanović M, Alagić S, Grekulović V, Trujić V (2013) Formulation and characterization of electrolyte for decorative gold plating based on mercaptotriazole. *Electrochim Acta* 104:330–336. <https://doi.org/10.1016/j.electacta.2013.04.123>
- Dimitrijević SB, Rajčić-Vujanović M, Jančić-Hajneman RM et al (2014) Temperature effect on decorative gold coatings obtained from electrolyte based on mercaptotriazole-comparison with cyanide. *Int J Mater Res* 105:272–281. <https://doi.org/10.3139/146.111017>
- Dimitrijević S, Stević Z, Rajčić-Vujanović M, Grekulović V, Dimitrijević S, Trumić B, Alagić S (2015) The influence of novel organic gold complex on photoresist layer of printed circuit board. *Metall Mater Eng* 21:269–275
- Dimitrijević SB, Rajčić-Vujanović MM, Jančić-Hajneman RM, Bajat JB, Trujić VK, Trifunović DD (2016) Microhardness of decorative gold coatings obtained from gold complex based on mercaptotriazole: comparison with cyanide. *Int J Mater Res* 107:624–630. <https://doi.org/10.3139/146.111382>
- Dimitrijević SB, Rajčić-Vujanović M, Dimitrijević SP, Trumić B, Ivanović A (2018) Stability of gold complex based on mercaptotriazole in acid and neutral media. *Bulg Chem Commun* 50:50–57
- Dimitrijević SB, Alagić SČ, Rajčić-Vujanović MM, Dimitrijević SP, Ivanović AT (2019) IR/Raman characterization of Au-mercaptoptriazole crystals. *Bulg Chem Commun* 51:358–364. <https://doi.org/10.34049/bcc.51.3.5003>
- Dimitrijević SB, Dimitrijević SP (2021). E-scrap processing: theory and practice, In: Gadov, Rainer and Mitic, Vojislav V. *Advanced Ceramics and Applications*, Walter de Gruyter GmbH, Berlin, Boston, pp 237–262. <https://doi.org/10.1515/9783110627992>
- Đorđević S, Maksimović M, Pavlović M, Popov K (1998) Galvanotehnika. Tehnicka knjiga, Beograd, pp 87–110 (in Serbian)
- Đorđević S (1990) Metalne prevlake. Tehnicka knjiga, Beograd, pp 295–298 (in Serbian)
- Garcia JC, Burleigh TD (2013) The beginnings of gold electroplating. *Electrochem Soc Interface* 22:36–38. <https://doi.org/10.1149/2.F02132if>
- Green TA (2007) Gold electrodeposition for microelectronic, optoelectronic and microsystem applications. *Gold Bull* 40:105–114. <https://doi.org/10.1007/BF03215566>
- Green TA, Roy S (2006) Speciation analysis of Au(I) electroplating baths containing sulfite and thiosulfate. *J Electrochem Soc* 153:C157–C163. <https://doi.org/10.1149/1.2164724/pdf>
- Hemsley SJ, Green RV (1991) The influence of bath components on deposit and operational characteristics in hard acid gold plating solutions. *Trans IMF* 69:149–153. <https://doi.org/10.1080/00202967.1991.11870912>
- Holm SC, Straub BF (2011) Synthesis of N-substituted 1,2,4-triazoles. A review. *Org Prep Proced Int* 43:319–347. <https://doi.org/10.1080/00304948.2011.593999>
- Honma H, Hagiwara K (1995) Fabrication of gold bumps using gold sulfite plating. *J Electrochem Soc* 142:81–85. <https://doi.org/10.1149/1.2043948/pdf>
- Hosseini M, Ebrhimi S (2010) The effect of Tl(I) on the hard gold alloy electrodeposition of Au–Co from acid baths. *J Electroanal Chem* 645:109–114. <https://doi.org/10.1016/j.jelechem.2010.04.013>
- Inoue T, Io S, Okudaira H, Ushio J, Tomizawa A, Takehara H, Shimazaki T, Yamamoto H, Yokono H (1999) In: Proceedings of the 45th IEEE electronic components technology conference, pp 1059–1067
- Ji Ram V, Sethi A, Nath M, Pratap R (2019) Five-membered heterocycles. In: Ji Ram V, Sethi A, Nath M, Pratap R *The chemistry of heterocycles*, Elsevier, pp 149–478. <https://doi.org/10.1016/B978-0-08-101033-4.00005-X>
- Jin L, Liu C, Yang FZ, Wu DY, Tian ZQ (2019) Coordination behavior of theophylline with Au(III) and electrochemical reduction of the complex. *Electrochim Acta* 304:168–174. <https://doi.org/10.1016/j.electacta.2019.02.118>
- Kato M, Okinaka Y (2004) Some recent developments in non-cyanide gold plating for electronics applications. *Gold Bull* 37:37–44. <https://doi.org/10.1007/BF03215515.pdf>
- Kato M, Sato J, Otani H, Homma T, Okinaka Y, Osaka T, Yoshioka O (2002) Substrate (Ni)-catalyzed electroless gold deposition from a noncyanide bath containing thiosulfate and sulfite: I reaction mechanism. *J Electrochem Soc* 149:C164–C167. <https://doi.org/10.1149/1.1448502>
- Krulik GA, Mandich NV (1993) *Metallic coatings*. Kirk-Othmer encyclopedia of chemical technology, 4th edn. Wiley, NY, pp 258–291
- Liew MJ, Roy S, Scott K (2003) Development of a non-toxic electrolyte for soft gold electrodeposition: an overview of work at University of Newcastle upon Tyne. *Green Chem* 5:376–381. <https://doi.org/10.1039/B301176N>
- Luo G, Li D, Yuan G, Li N (2018) Communication—a cyanide-free electrolyte for hard gold (Au–Co) electrodeposition utilizing DMH as complexing agent. *J Electrochem Soc* 165:D107. <https://doi.org/10.1149/2.0291803jes>
- Okinaka Y, Hoshino M (1998) Some recent topics in gold plating for electronics applications. *Gold Bull* 31:3–13. <https://doi.org/10.1007/BF03215469>
- Osaka T, Okinaka Y, Sasano J, Kato M (2006) Development of new electrolytic and electroless gold plating processes for electronics applications. *Sci Technol Adv Mater* 7:425–437. <https://doi.org/10.1016/j.stam.2006.05.003>
- Qu J, Huang SF, Zhou MJ, Li L, Li C, Geng HD (2014) The effects of additives on the properties of non-cyanide electroless gold plating deposition. *Adv Mat Res* 1030–1032:205–208
- Rapson WS, Groenewald T (1978) *Gold usage*. Academic Press, London, pp 196–270
- Remko M, Rode BM (2006) Effect of metal ions (Li⁺, Na⁺, K⁺, Mg²⁺, Ca²⁺, Ni²⁺, Cu²⁺, and Zn²⁺) and water coordination on

- the structure of glycine and zwitterionic glycine. *J Phys Chem A* 110:1960–1967. <https://doi.org/10.1021/jp054119b>
- Richter F, Gesemann R, Gierth L, Hoyer E (1989). German Patent DD268484
- Roy S (2009) Electrochemical gold deposition from non-toxic electrolytes. *ECS Trans* 16:67–72. <https://doi.org/10.1149/1.3114009/pdf>
- Sato J, Kato M, Otani H, Homma T, Okinaka Y, Osaka T, Yoshioka O (2002) Substrate (Ni)-catalyzed electroless gold deposition from a noncyanide bath containing thiosulfate and sulfite: II. Deposit characteristics and substrate effects. *J Electrochem Soc* 149:C168. <https://doi.org/10.1149/1.1448503>
- Sullivan A, Kohl P (1997) Electrochemical study of the gold thiosulfate reduction. *J Electrochem Soc* 144:1686–1690. <https://doi.org/10.1149/1.1837660/pdf>
- Traut J, Wright J, Williams J (1990) Gold plating optimization for tape automated bonding. *Plat Surf Finish* 77:49–53
- Wrzosek B, Bukowska J (2007) Molecular structure of 3-amino-5-mercaptopto-1, 2,4-triazole self-assembled monolayers on Ag and Au surfaces. *J Phys Chem* 111:17397. <https://doi.org/10.1021/jp075442c>
- Xingkai Z, Qingyi Q, Li Q, Bin Z, Junyan Z (2020) Comparison study of gold coatings prepared by traditional and modified galvanic replacement deposition for corrosion prevention of copper. *Microelectron Reliab* 110:113695. <https://doi.org/10.1016/j.microrel.2020.113695>

Publisher's Note Springer Nature remains neutral with regard to jurisdictional claims in published maps and institutional affiliations.

Springer Nature or its licensor holds exclusive rights to this article under a publishing agreement with the author(s) or other rightsholder(s); author self-archiving of the accepted manuscript version of this article is solely governed by the terms of such publishing agreement and applicable law.